

Techno-economic optimization and analysis of a high latitude solar district heating system with seasonal storage, considering different community sizes

Janne Hirvonen*, Hassam ur Rehman, Kai Sirén

Aalto University, School of Engineering, Department of Mechanical Engineering, P.O. Box 14400, FI-00076 Aalto, Finland

ARTICLE INFO

Keywords:

Solar community
Simulation-based optimization
Energy system scaling
Seasonal storage
Solar district heating
Solar assisted heat pump

ABSTRACT

A solar community meets a significant amount of its energy demand through solar energy. In a high latitude country like Finland, the seasonal mismatch of solar availability makes it very difficult to achieve high renewable energy fractions without seasonal storage. In this study, a solar community located in Finland was optimized with respect to energy demand and life cycle cost. To gain better understanding of both technical and economical scaling effects, the optimization was done separately for four cases with 50, 100, 200 and 500 buildings.

The study was performed for Finnish conditions using dynamic TRNSYS simulations and optimized with a genetic algorithm, using the MOBO optimization tool. The modeled energy system had solar thermal collectors and solar electric panels for energy generation, two centralized short-term storage tanks and a seasonal borehole thermal energy storage system (BTES) for energy storage, and a ground source heat pump for additional heat generation.

The larger communities provided noticeable cost-benefits when aiming for high performance. Larger seasonal storages allowed more direct utilization of seasonally stored heat, lowering the need for the heat pump and reducing electricity demand. Comparing the best and worst performing optimal energy system, annual demand for heating electricity was reduced by 80%. Renewable energy fractions close to 90% for heating were possible for all community sizes, but the large communities could obtain them with about 20% lower costs.

1. Introduction

The heating of buildings is a large part of the total European energy demand, especially so in the Nordic countries. For example, in Finland, 87% of energy is consumed by heating (Statistics Finland, 2014). Producing heating through emissions-free renewable energy systems would lower its environmental impact. Such systems might be based on biomass or hybrid solar heating (Modi et al., 2017). Solar energy is a widely available energy source, but suffers from both diurnal and seasonal variation. The diurnal variation is a significant problem for solar electric systems, because of the hourly mismatch between energy generation and demand and the high cost of electricity storage. However, thermal energy storage in hot water tanks is a very mature technology and mostly removes the hourly mismatch in heating applications. It can even partly solve the hourly solar electricity mismatch problem (Hirvonen et al., 2016). Unfortunately, home-scale hot water tanks are of little use in solving the problem of seasonal mismatch, where the heating energy demand is the highest exactly when the solar generation is the lowest, during winter (Fig. 4). This problem is especially difficult

in high latitude countries, because the relative difference between summer and winter solar energy availability increases the further we move from the equator.

The problem of seasonal variation can be solved through seasonal thermal energy storage (Xu et al., 2014). Using seasonal storage, energy can be stored in the peak months to be used during times of high energy demand. While technologies are being developed for chemical and latent heat storage, existing seasonal storage systems mostly utilize sensible heat storage, based on changing the temperature of a high heat capacity material. The basic storage types in this group are hot water tank thermal energy storage (TTES), aquifer thermal energy storage (ATES), water pit thermal energy storage (PTES) and borehole thermal energy storage (BTES).

Seasonal thermal energy storage is often utilized in solar communities, where the goal is to meet a significant part of the heating demand by solar energy, that is, to achieve a high solar fraction. The history of solar communities began in the 1970s energy crisis (Reuss, 2015). Many such communities have been built in Europe in the 1980s, 1990s and 2000s, mostly in Denmark (Heller, 2000), Germany (Schmidt

* Corresponding author.

E-mail address: janne.p.hirvonen@aalto.fi (J. Hirvonen).

Nomenclature

Symbol/acronym

BTES	borehole thermal energy storage
DLSC	Drake Landing Solar Community
DHW	domestic hot water
HP	heat pump
PV	photovoltaics
SH	space heating
ST	solar thermal
A_{floor}	heated floor area (m^2)

A_{ST}	solar thermal area (m^2)
h_{ratio}	BTES height vs. width ratio (m/m)
LCC	life cycle cost over 25 years ($\text{€}/\text{m}^2$)
$N_{\text{boreholes}}$	number of boreholes in BTES (–)
N_{series}	number of boreholes connected in series (–)
REF_{heat}	renewable energy fraction of heating (–)
$\text{REF}_{\text{total}}$	Renewable energy fraction of total electricity (–)
SF	Solar fraction (–)
SPF	Seasonal performance factor of heating ($\text{kW h}/\text{kW h}$)
V_{BTES}	Seasonal storage volume (m^3)
α_{tilt}	Tilt angle of solar collectors ($^\circ$)
$\rho_{\text{boreholes}}$	Area density of boreholes in BTES ($1/\text{m}^2$)

et al., 2004) and Sweden (Lundh and Dalenbäck, 2008). Some of the projects store energy into the ground (BTES), but water-based storage with tanks have also been studied (Tulus et al., 2016). While current efforts in Denmark are towards large solar district heating systems based on water pit storage (Ramboll, 2015), existing solar communities are of many different sizes, as shown in Fig. 1a.

The German Neckarsulm community consists of 200 apartments and a shopping center, school and gym, built in 1997 (Nussbicker et al., 2004). It has a $63\,000\text{ m}^3$ BTES system with a gas boiler and heat pump for backup. The Crailsheim community of similar scale was built in 2007 and has a $37\,500\text{ m}^3$ BTES storage that serves 260 apartments, a school and a gym (Bauer et al., 2010). Backup heating was handled by district heat and a heat pump. The seasonal storage was smaller in Crailsheim than Neckarsulm, but the amount of solar collectors was larger, 7500 m^2 compared to 5670 m^2 . The Attenkirchen solar community is much smaller, serving only 30 homes (Reuss et al., 2006). This system utilizes an underground water tank, surrounded by a $10\,500\text{ m}^3$ BTES system. Similar design was used in the only Finnish solar community trial in Kerava (Lund, 1984), though the system was later dismantled and replaced by conventional district heating.

Perhaps the most famous solar community is the Drake Landing Solar Community (DLSC) in Canada, which started operation in 2008 (Sibbitt et al., 2011). It utilizes 2300 m^2 of solar collectors, two water-based buffer storage tanks and $34\,000\text{ m}^3$ BTES system to supply heating to 52 houses. A system of similar scale is the Swedish Anneberg solar community, with a $60\,000\text{ m}^3$ BTES volume and a 2400 m^2 solar thermal area. The DLSC system has been able to meet 98% of space heating demand through solar energy, while the Anneberg system

supplies about 60% of combined space heating and domestic hot water (DHW) demand (Zhu, 2014). On the other extreme of solar communities is the Braedstrup solar district heating system in Denmark (SDH EU, 2012). It was built in 2007 and extended in 2012 to have a $19\,000\text{ m}^3$ BTES volume with an $18\,600\text{ m}^2$ solar thermal area. The system is backed up by an electric boiler and a heat pump and supplies heat to 1200 homes. Because of the large heat demand compared to the solar thermal capacity, the solar fraction is only 20%, but this also ensures minimal waste of available solar energy.

Every solar community has a different amount of buildings, different sizes of short-term and long-term energy storage as well as different solar collector areas, different auxiliary heating systems and different environmental conditions. Thus, even when the communities report different solar fractions, it is hard to tell what is the main reason for the performance. Fig. 1b shows the solar fractions achieved by solar communities, arranged according to their ratio of energy storage to solar capacity and ratio of solar capacity to heated space. All of these systems utilize BTES for their seasonal storage needs. It seems that the highest solar fractions have been achieved by systems with more solar thermal capacity per heated area and more storage capacity per solar thermal capacity. The opposite also holds true for the smallest solar fraction. However, for most samples the correlation is far from clear, which implies other factors are also important.

This article examines the effect of community size on the techno-economic optimization of a high latitude solar community in a heating-dominated climate. Specific environmental challenges include high seasonal variability of solar energy and highly conductive ground. Total system optimizations have not been widely reported in the literature.

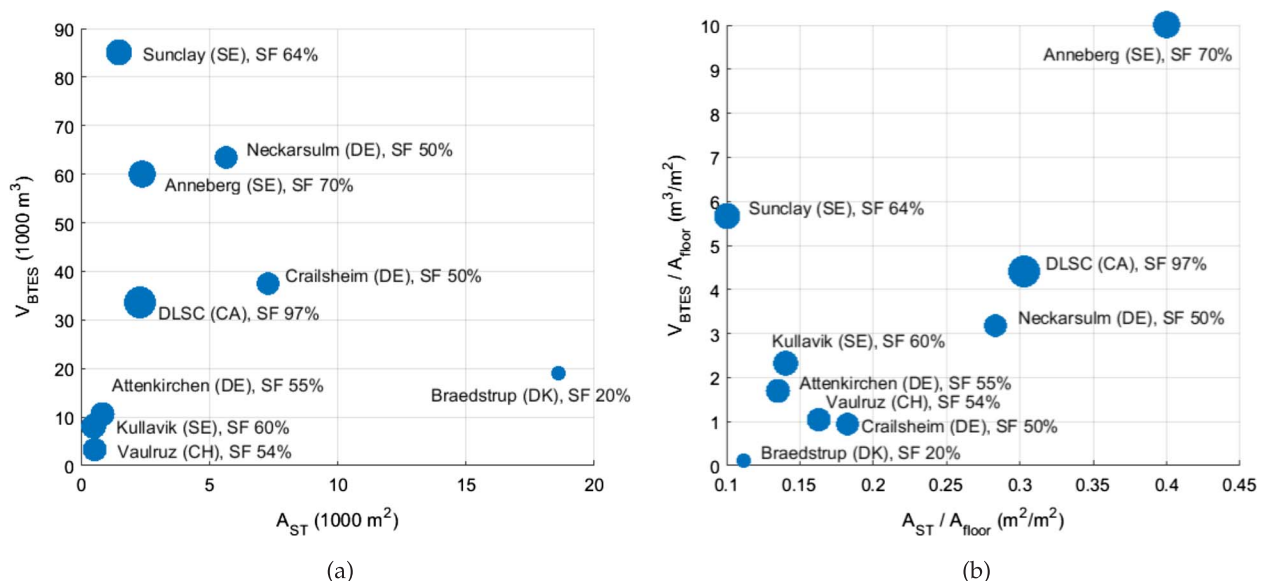


Fig. 1. (a) Solar fraction of some realized solar communities. (b) Solar fraction reported with relative system sizes.

The focus is specifically on Finland, as actual solar community projects have not been materialized there like in other Nordic countries. However, neighbouring countries Sweden, Norway and Estonia share a similar climate which increases the applicability of the results. The work is done by multi-objective optimization with a genetic algorithm, using life cycle cost and energy performance as objectives. Different energy storage and generation configurations are considered, along with efficiency improvements. The aim is to see if community size has an influence on which features are dominant and to increase understanding of system design to help realize actual projects in the near future.

2. Materials and methods

2.1. Energy system details and modeling

The solar community under study consisted of a simulated group of 100 m² single-family detached houses, which were connected to a local heating grid. The buildings were assumed to be located in southern Finland (60°N). The energy system was modeled in TRNSYS 17. Solar thermal collectors (ST) and solar photovoltaic panels (PV) were located on the roofs of each building. The solar thermal system was connected to a centralized heat storage system, containing two water-based short-term storage tanks (high and low temperature) and a borehole thermal energy storage (BTES) system (Type 557a). The design of the system is shown in Fig. 2. The solar collectors were connected to both tanks in parallel, so each could be charged according to current temperature levels. The low temperature tank, which was kept at close to 40 °C, was used for supplying space heating (SH) and for preheating domestic hot water (DHW). The high temperature tank, which was kept at above 60 °C, was used for boosting the DHW to the minimum temperature of 55 °C required by the Finnish building code (Finlex, 2007). The solar thermal output was used to keep the hot tank at the required temperature, otherwise the flow was directed to the low temperature tank. If the tank temperature rose 10 °C above the setpoint, the energy in the

tank was discharged into the seasonal storage until the tank had cooled down enough. Solar thermal collectors were modeled based on Savo-Solar rooftop collectors (Solar Keymark Database, 2013). The flowrate to the solar collectors was controlled to keep the temperature output at 1 °C higher than the top of the target thermal storage tank. Either tank could be charged, depending on the current storage temperatures.

The seasonal storage was a borehole thermal energy storage (BTES), where the boreholes were evenly distributed along the top surface area. Each borehole was fitted with U-tube piping which served as a heat exchanger between the ground and the heat transfer fluid. Several boreholes could be connected in series so that the fluid exiting from one borehole could be pumped into the next one. In charging mode, hot fluid was pumped into the center of the storage and the cooled output flow was directed into the next borehole in series. Thus, a radial temperature distribution could be formed, where the center of the storage had the highest temperature and the edges had the lowest, minimizing heat losses to the surroundings. The flowrate in each borehole loop was set to 400 kg/h, but if during charging the tank temperatures rose too high, the flowrate was doubled to prevent the tank from overheating.

When the temperature in the tanks was too low, they were charged from the BTES. In this mode, the cold fluid entered from the cool outer edge and exited from the hot center. Whenever possible, the flow from BTES was used to heat the tanks directly, but if the temperature was not high enough it was instead used as the heat source for heat pumps. The high temperature of the ground circuit significantly increased the COP, as shown in Fig. 3. Direct electric heaters were used for backup heating. If the ground was cooled to below −5 °C, the heat pump was deactivated and heating was handled by the direct electric heaters. If the source temperature for the heat pump was above 30 °C, the source flow was assumed to be mixed with the cooled return flow, so that the heat pump COP matches the maximum values shown in Fig. 3.

Cooling and space heating demands in the building were based on TRNSYS simulations with Type 56. Different building configurations were simulated independently of the solar community, using different options of windows, insulation and heat recovery efficiency. Seven

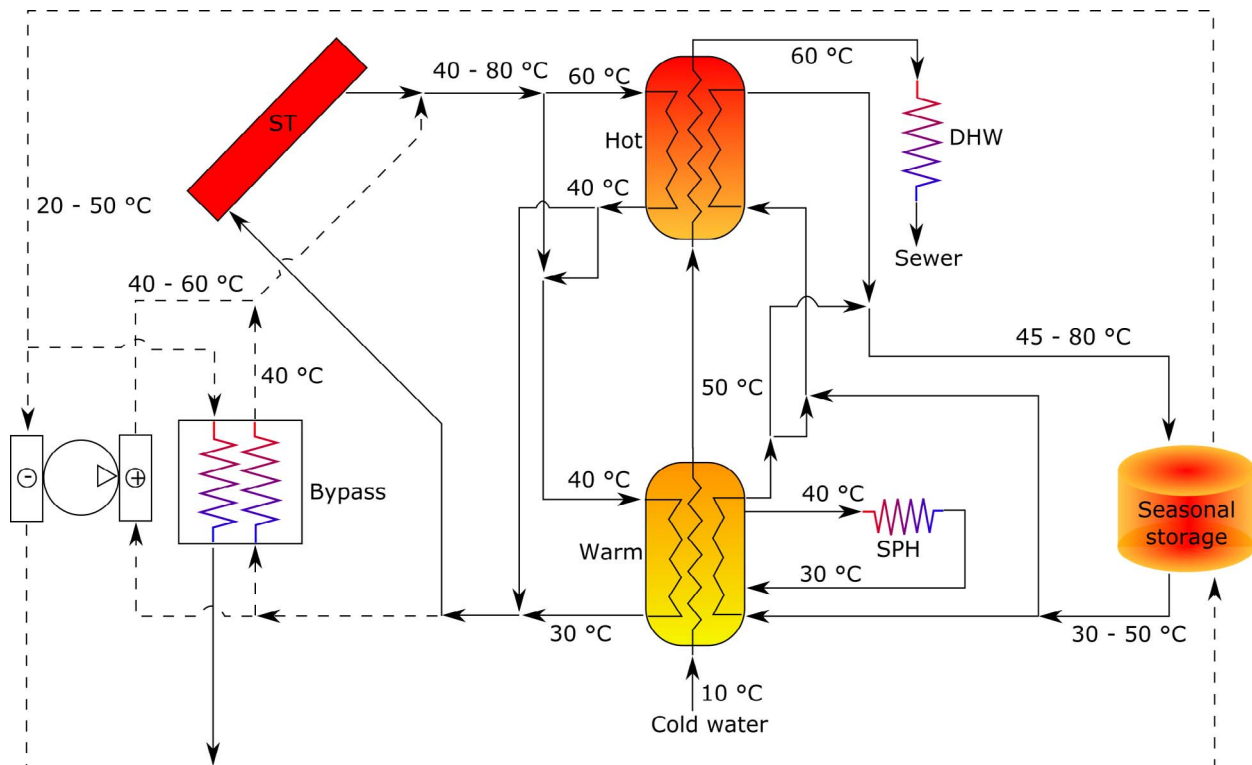


Fig. 2. The heating system consisted of solar thermal collectors, two buffer tanks, a borehole seasonal energy storage and a heat pump. Parallel connection allowed solar collectors to charge either tank separately, while series connection treated them as a single tank.

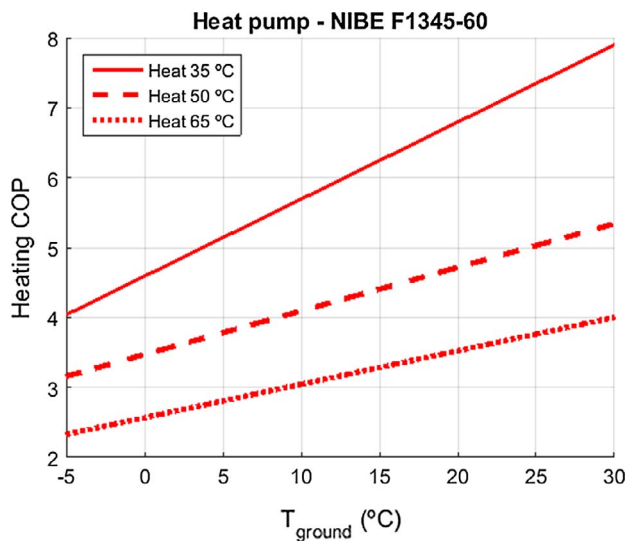


Fig. 3. The COP of the heat pump increases until the source temperature reaches 30 °C. Above that point the inlet flow was assumed be mixed with cooled return fluid so that the COP remained constant.

Pareto optimal building configurations (in terms of cost and energy efficiency) were used as options for the total system optimization, where LCC and external electricity use of the community were similarly minimized. The annual space heating demand with respect to floor area in the buildings varied from 25 kWh_{th}/m² to 50 kWh_{th}/m² (Fig. 7). Due to the low cooling needs of the community, no cooling system was included.

The DHW flow profile was based on IEA data (Jordan and Vajen, 2001). Several copies of the same profile were shifted by 0 to 5 weeks and 0–2 h to provide an aggregation effect where the weekdays remain the same, but slight differences to hourly scheduling appear. The basic annual DHW demand in the buildings was 35 kWh_{th}/m², but to guarantee quick access to hot water the simulation included constant circulation of hot water, even when there was no actual demand, which increased the effective use to 42 kWh_{th}/m². Additionally, the demand profile for lighting and appliances was a normalized aggregate of measured demand from 50 buildings in the Helsinki region, provided by the Fortum company (Fortum Oy, 2015). For privacy reasons, no other information about the houses was provided and the aggregated profile was thus normalized to 40 kWh_{el}/m² annual electricity demand, according to measurements of a low-consumption house where size data

was available.

Fig. 4 shows the monthly heating demand per heated floor area and the solar insolation for a surface sloped at 40°. DHW demand remains roughly constant through the year, while SH demand goes to zero during the summer. The figure also shows the difference in SH demand in the best and worst quality houses, with the space heating demand for all seven building configurations lying between the minimum and maximum values. The seasonal mismatch between demand and generation is evident, along with the large difference between the minimum and maximum solar generation.

The weather data used for the simulation was the Helsinki Test Reference Year 2012 (Kalamees et al., 2012), with annual horizontal solar insolation of 975 kWh/m². The BTES was located on a rocky Finnish ground, with an average thermal conductivity of 3.50 W/mK. The volumetric heat capacity was 2240 kJ/m³ K (Flynn and Sirén, 2015). Because the BTES system required several years to heat up and achieve optimal performance, it was not enough to run the simulation for just one year, but due to long simulation time, 25 year simulation was also not considered feasible. As a compromise, the system was simulated for 4 years and the fourth year was used to estimate the cost and performance for all the remaining years.

2.2. Performance indicators

The performance of a solar community can be evaluated by examining its final demand for imported off-site energy. However, some other indicator can also be useful for comparing case studies. Solar fraction (SF) is a common indicator that describes the fraction of energy demand met by solar energy. The solar fraction is also known as the renewable energy fraction or the on-site energy fraction (Cao et al., 2013). In this study, the solar energy system is supported by a ground-source heat pump, which means that energy can be taken out of the storage even if it has not been charged with active solar systems. Thus, to avoid confusion, this study uses the renewable energy fraction (REF) as a performance indicator. REF was defined separately for heating and total electricity demand. Due to utilizing both short-term and long-term thermal storage, as well as heat pumps, the total solar energy generation couldn't be used for the calculation directly, because there were significant thermal losses and energy conversion from electricity to heat. Instead, REF was calculated indirectly by determining the electricity consumption of all heating-related systems (HP, pumps, backup heating) and assuming all remaining energy was generated by solar energy. For heating, REF was defined using the ratio of electricity needed to run the heating system vs. the total heat demand met by the

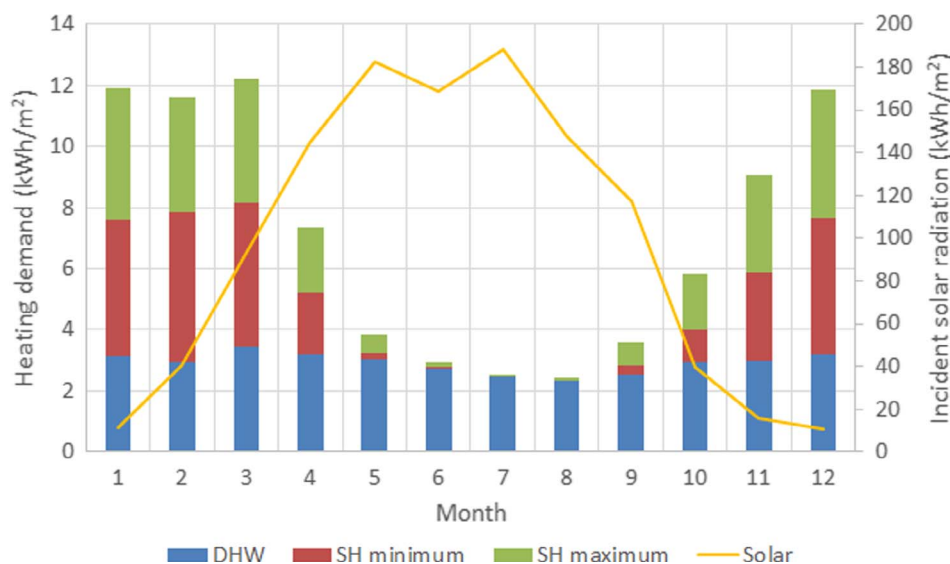


Fig. 4. Monthly heating energy demand as thermal energy. Space heating demand is split into two parts: the minimum corresponds to the most efficient building configuration 7, while the maximum corresponds to the least efficient building configuration 1 (Fig. 7). Solar insolation is given for south-facing collectors tilted at a 40° angle.

system

$$REF_{\text{heat}} = 1 - \frac{E_{\text{heating}}}{E_{\text{heat,dem}}} = 1 - \frac{E_{\text{pumps}} + E_{\text{HP}} + E_{\text{backup}}}{E_{\text{SH}} + E_{\text{DHW}}}, \quad (1)$$

where E_{heating} is the electricity needed to run the heating system, $E_{\text{heat,dem}}$ is the total heating energy used in the buildings, E_{pumps} , E_{HP} and E_{backup} are the electricity use of the pumps, heat pump and backup heating, respectively, and E_{SH} and E_{DHW} are the actual amount of heat used to provide space heating and domestic hot water.

Eq. (1) indirectly takes into account both the direct-use and ground-stored solar energy, as their inclusion lowers the need for direct electric backup heating and heat pump compressor operation (which is denoted by E_{HP}). Solar electricity was not considered in the calculation of REF_{heat} .

Since grid electricity was the only external energy source, the REF for the whole system was defined using the ratio of annually imported electricity vs. the total electricity demand

$$REF_{\text{total}} = 1 - \frac{E_{\text{elec,import}}}{E_{\text{elec,dem}}} = 1 - \frac{E_{\text{heating}} + E_{\text{appliances}} - E_{\text{PV-self-consumption}}}{E_{\text{heating}} + E_{\text{appliances}}}, \quad (2)$$

where $E_{\text{elec,import}}$ is the electricity imported from the grid, $E_{\text{elec,dem}}$ is the total electricity use by the buildings, $E_{\text{appliances}}$ is the energy demand of lights and other non-heating appliances and $E_{\text{self-consumption}}$ is the amount of locally generated solar electricity that is used on-site (not exported as excess). Excess solar energy is sold to the grid for small profit, but it does not compensate for demand in other time periods.

The efficiency of a seasonal energy storage system can be defined simply as the ratio of annual energy taken out of the BTES vs. solar energy injected into the storage (Flynn and Sirén, 2015)

$$\eta_{\text{BTES}} = \frac{E_{\text{discharge}}}{E_{\text{charge}}}. \quad (3)$$

This efficiency measure is dependent on both the storage and energy generation system performance and can sometimes give unexpected results. For example, if there is not enough heat injected into the system, the annual discharging may exceed charging, giving an efficiency greater than 1. When this happens, the storage is either recharged naturally from the surrounding ground or the BTES is permanently cooled, eventually making it unusable for geothermal energy applications.

2.3. Economic parameters

The life cycle cost (LCC) was formed out of the initial investment cost and the operation cost (cost of imported electricity) during 25 years. Discounting was done with a real interest rate of 3% (EU-Commission, 2012). The hourly electricity price was the sum of the Nord Pool spot price (Nord Pool, 2016), the distribution price of the local network operator and the Finnish electricity tax (Caruna Oy, 2016). The average prices (including VAT) were 5.5, 4.0 and 2.8 c €/kWh, respectively. The total cost for buying electricity was thus approximately 12 c€/kWh. The value of self-consumed PV electricity was equal to the total buying price. However, when selling excess electricity to the grid, the value was equal to only the spot price. Hourly spot price profiles from the years 2010 to 2014 were used cyclically, so that each profile repeated every five years. Due to the reversing price trend in the Nordic electricity market, the average price increase during the past decade has been low and even negative (Nord Pool, 2016). Thus, a conservative electricity price escalation rate of 1% was used in this study.

A constant unit price was used for some energy system components (Table 1). For other components, the price was assumed to go down with larger amounts. These include the solar thermal collectors (Fig. 5), PV panels (Fig. 5) and tanks (Fig. 6). Lowering relative price results from economies of scale, as fixed costs may be independent of system

capacity and production efficiency improves by making larger production runs and through worker learning. Companies can also profit, if they can sell more even with a slightly lower price. The price for improving the energy performance of buildings was given as the difference against the worst performing building configuration (Fig. 7). Costs of building efficiency components are reported in Table 2 and the optimal building configurations are shown in Table 3.

2.4. Optimization problem

The goal of the optimization was to minimize both imported electricity and life cycle cost (LCC). The problem was defined as

$$\begin{aligned} \min \{f_1(x), f_2(x)\} \\ \text{s.t. } g(x) = A_{ST} + A_{PV} \leq 60 \text{ m}^2 \\ lb_i \leq x_i \leq ub_i, \quad i \in \{1, \dots, 14\}, \end{aligned} \quad (4)$$

where f_1 is the amount of annually imported electricity, f_2 is the life cycle cost, g is the limit on roof space and lb_i and ub_i are the lower and upper bounds for all decision variables. The decision variables are introduced in Table 4. The life cycle cost was the sum of initial investment cost and the discounted operation cost over 25 years.

Four different community sizes were used: 50, 100, 200 and 500 buildings. A separate optimization was performed for each community size. Optimization was performed with the MOBO optimization tool (Palonen et al., 2013), using a Pareto archive genetic algorithm (Hamdy et al., 2012). Population size was 24, crossover probability 0.9 and mutation probability 0.07. Additional calculations during optimization were performed with MATLAB.

3. Results

3.1. Optimization results

The results of the optimization for all community sizes are shown in Fig. 8. When increasing the community size from 50 to 200 buildings, the same performance was obtained with lower cost. Further size increase to 500 buildings provided no additional cost benefit. It is clear that lower unit costs of larger systems should provide some economical benefits, but are there other factors in play as well? Are there some pure performance benefits or specific features that follow from larger system size? All the following analysis is based on the near-optimal solutions shown in Fig. 8. Many figures show the results with respect to imported electricity, which means the total electricity demand of heating and appliances after self-consumption of PV power has been subtracted. Excess solar electricity generation was sold for profit, but did not affect the net energy balance.

Table 5 shows the features and performance of some Pareto optimal solutions for each community size. They were chosen based on LCC, so that each size category has three cases of similar cost. This helps to illustrate differences in performance and cost distribution. We can note that the short-term storage capacity increases when aiming for high performance. On the other hand, large seasonal storage volumes were connected with the lowest performance. When the community size increases, a high performance seems to require less boreholes per building. There were 7 different options for the building energy performance (1 having the worst performance and 7 the best) and most

Table 1
Energy system components with constant unit prices.

System component	Price	Unit
HP (Haahtela and Kiiras, 2013)	325	€/kW
Borehole drilling (Haahtela and Kiiras, 2013)	33.5	€/m
BTES excavation (Rakennuslehti, 2016)	3.0	€/m ³
BTES insulation (Rautia, 2016)	88	€/m ³

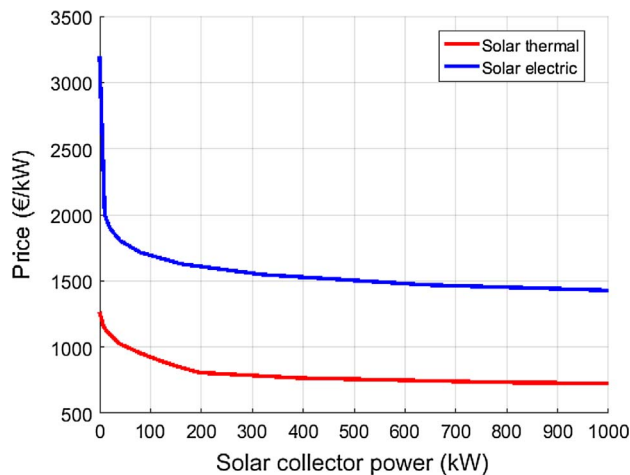


Fig. 5. Cost of rooftop solar thermal (Mauthner, 2016) and solar electric (Ahola, 2015) systems. Prices are given as €/KW_{th} and €/KW_{el}, respectively. Solar thermal power estimated at 10 K temperature difference.

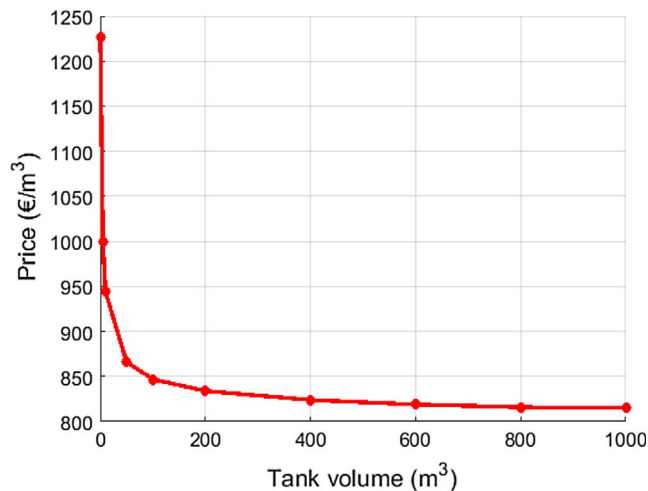


Fig. 6. Cost of short-term thermal storage tanks (Mauthner, 2016).

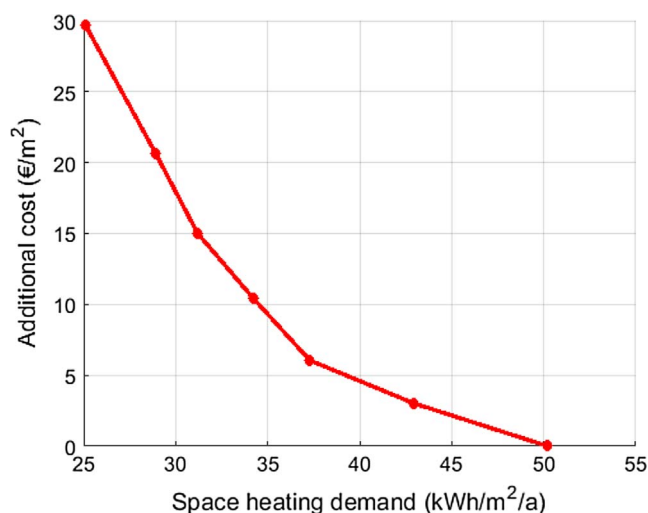


Fig. 7. Additional cost (per floor area) of building energy efficiency improvements relative to the lowest performing building. These include different levels of insulation, window quality and heat recovery efficiency as shown in Tables 2 and 3.

Table 2

Cost of building efficiency components (Hamdy et al., 2013; Haahtela and Kiiras, 2013).

Component	Details	Price	Unit
Wall insulation	Mineral wool	62.7	€/m ³
Roof insulation	Blow-in wool	36.2	€/m ³
Floor insulation	Polyurethane	111.4	€/m ³
Windows	U-value 0.98 W/m ² K	195	€/m ²
	U-value 0.8 W/m ² K	221	
	U-value 0.6 W/m ² K	270	
Ventilation heat recovery efficiency	Cross-flow HX, $\eta = 60\%$	3533	€/house
	Counter-flow HX, $\eta = 70\%$	3835	
	Regenerative HX, $\eta = 80\%$	4138	

Table 3

Optimal building configurations.

Configuration	SH demand (KW h/m ²)	Insulation and window U-values				Heat recovery efficiency (%)
		Wall (W/m ²)	Floor (W/m ²)	Roof (W/m ²)	Windows (W/m ²)	
1	50.2	0.17	0.17	0.09	0.98	60
2	43.0	0.17	0.17	0.09	0.98	70
3	37.3	0.17	0.17	0.09	0.98	80
4	34.2	0.13	0.17	0.09	0.98	80
5	31.2	0.13	0.17	0.07	0.98	80
6	28.9	0.10	0.17	0.07	0.98	80
7	25.1	0.13	0.17	0.07	0.60	80

optimal configurations used building configuration 7. This indicates that minimizing energy demand has a higher priority than investing in energy generation and storage systems.

Fig. 9 shows the BTES efficiency with respect to the total purchased electricity consumption. On the high performance side (energy consumption between 30 and 35 kW h/m²), the larger communities had better efficiencies than the smaller ones as the efficiency increased from 40% in the 50 building case, to 55% in the 100 building case and up to 70% in the 500 building case. This matched with expectations, but for much of the samples there was no clear difference in BTES efficiency that could be attributed to the community size. For all sizes, a clear trend is visible, as storage efficiency decreased while total system performance improved. This can be attributed to the increased storage temperatures resulting from larger ST capacities.

BTES efficiency as defined in Eq. (3) can be misleading, as evidenced by the points where the efficiency is greater than 1. These situations occur when the solar heating system is undersized and heat pumps drain so much energy from the ground that it will cool down below the temperature of the surrounding ground. When this happens, the BTES is naturally regenerated like a conventional GSHP system and the BTES efficiency increases. Thus, BTES efficiency is highest when solar energy injection is minimal. To enhance readability, abnormally high efficiencies that were greater than 10 are not shown in the figure, even though such cases occurred in the case of 50 buildings when solar thermal capacity was less than 10 m².

BTES efficiency values were related to the shape of the seasonal storage. Fig. 10 shows the height-to-width ratio for the optimal cases with all community sizes. With 50, 100 and 500 buildings, the height-to-width ratio was high when the system performance was poor. This means that the seasonal storage is more deep than wide. This increases the heat transfer through the sides of the storage. When solar energy injection is low, a cooled down BTES will be charged naturally from the surrounding terrain. Performance improvement was generally tied to a decreasing height-to-width ratio. The BTES can be insulated from the top, which benefits wide designs with a low height-to-width ratio. A wide shape also allows the BTES core to obtain higher temperatures.

Table 4
Decision variables for optimization.

Decision variable	Lower bound	Upper bound	Unit	Variable type	Description
A_{ST}	2	40	$m^2/\text{building}$	Continuous	Solar thermal collector area on each roof
V_{hot}	0.5	5.0	$m^3/\text{building}$	Continuous	Hot buffer tank size
V_{warm}	0.5	5.0	$m^3/\text{building}$	Continuous	Warm buffer tank size
A_{pv}	0	60	$m^2/\text{building}$	Continuous	Solar electric panel area on each roof
h_{ratio}	0.25	5	-	Continuous	BTES height vs. width ratio
V_{BTES}	100	1000	$m^3/\text{building}$	Continuous	Volume of seasonal borehole storage
$d_{insulation,BTES}$	0	2	m	Continuous	Thickness of BTES top insulation
α_{tilt}	20	80	°	Continuous	Tilt angle of solar collectors and PV panels
$E_{building}$	25	50	$KW\ h/m^2/a$	Discrete	Space heating demand in buildings
N_{HP}	1	25	-	Discrete	Number of heat pumps (60 kW_{th})
$\rho_{boreholes}$	0.05	0.25	boreholes/ m^2	Continuous	Borehole density
N_{series}	1	9	-	Discrete	Number of boreholes in series

The decreasing height-to-width ratio can also be seen in Fig. 11. A wide shape has the added benefit that more boreholes can be installed, which can increase total flowrate. When there is little solar injection, the ground storage needs to be very large, to prevent freezing during heat pump operation, as can be seen in Fig. 12. In the low performance scenarios (over $45\ kW\ h/m^2$ electricity demand), a large community seems to need relatively less storage volume to obtain similar performance as a small community. In the case of 200 buildings, all optimal solutions had height-to-width ratios close to 1, even in the low performance cases. Clearly, BTES design is not the only factor that determines total system efficiency. The difference of the 200 building scenario can be explained by its higher solar thermal capacity (Fig. 13). Even in the low performance scenarios ($45\text{--}50\ kW\ h/m^2$) there was enough solar injection to allow the wide and small storage to be feasible. In the 50 and 100 building communities the lack of solar energy had to be compensated by a large storage with significant passive regeneration. In the 500 building community, both the average BTES size and solar capacity were between these two extremes. Some of the differences between the size categories can be explained by the random nature of genetic algorithms. Solutions generated by GA depend on both previous solutions and random changes and are not guaranteed to be optimal, though in practice they are usually nearly optimal.

As the size of the community was increased, the number of boreholes connected in series in the BTES decreased. The amount of seriality in the optimal cases is shown in Fig. 14. It was expected that having more seriality would improve total efficiency by increasing the BTES

output temperature and by lowering thermal losses through stronger radial temperature distribution. Indeed, this was the case in the 50 building scenario, as high performance was obtained using 4 to 9 boreholes in series. However, in the larger communities the number of series-connected boreholes was lower. Since the flowrate within each borehole loop was kept constant, parallel borehole connections allowed for a higher total flowrate, which increased the power transfer to and from the BTES. Despite the higher losses in the seasonal storage, this proved beneficial for the cost of operation in cases with 100, 200 and 500 buildings, as more of the heating demand could be met by direct utilization of seasonally stored heat, without heat pump operation. Having many boreholes connected in series increased the output temperature from the BTES. While this made it easier to directly utilize the stored heat, it also caused the output temperatures to be unnecessarily high, which could induce mixing losses when the low temperature tank was charged with unnecessarily hot fluids. Additionally, the heat pump gained no benefit from temperatures higher than $30\ ^\circ C$. It seems that strong seriality is only important for small BTES sizes.

One benefit of larger community size was that the relative amount of boreholes decreased. Fig. 15 shows the number of boreholes per house. The amount increased as performance improved, but the larger communities had lower average values. Drilling can be a significant cost, so the lower amount is a benefit for large communities. The number of boreholes does not tell the whole truth, however. Fig. 16 shows the combined length of all boreholes relative to the number of buildings. Here we see an opposite trend that the total borehole length

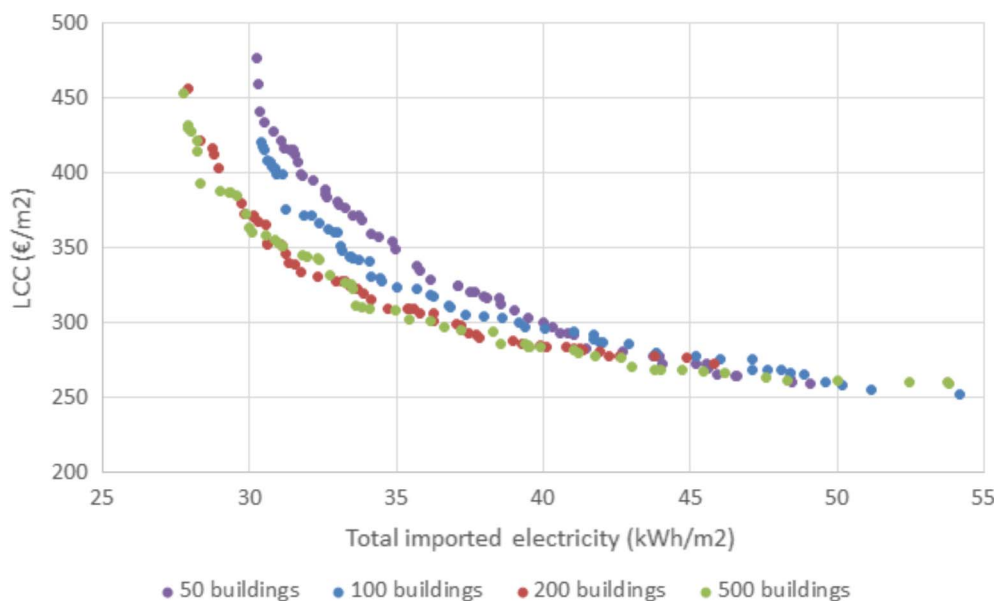


Fig. 8. Pareto optimal solutions for each community size, showing discounted life cycle cost during 25 years vs. the consumption of total imported electricity after PV self-consumption has been accounted for. The values are normalized to the total heated floor area of all buildings in the community.

Table 5
Features of some optimal solutions.

Buildings		50			100			200			500		
Category		A	B	C	A	B	C	A	B	C	A	B	C
Electricity use	kWh/m ²	45.6	36.2	31.7	47.1	34.1	30.9	45.8	32.3	28.9	43.0	32.7	28.3
LCC	€/m ²	269	329	399	269	330	399	273	331	403	270	332	393
SPF	kWh/kWh	3.1	5.3	8.1	2.9	5.5	8.3	3.0	6.8	11.3	3.3	7.3	13.2
REF _{heat}	–	0.68	0.81	0.88	0.65	0.82	0.88	0.67	0.85	0.91	0.70	0.86	0.92
REF _{total}	–	0.28	0.33	0.35	0.27	0.36	0.37	0.30	0.36	0.38	0.30	0.35	0.38
ST area	m ² /house	6.3	19.6	32.0	5.3	20.8	26.4	13.7	22.8	32.9	11.1	25.3	28.7
Hot tank volume	m ³ /house	0.6	1.7	1.0	0.7	1.7	4.2	0.7	1.8	3.0	0.5	0.6	3.5
Warm tank volume	m ³ /house	1.0	1.9	2.6	0.8	1.8	3.2	0.6	2.3	2.9	0.8	4.4	4.2
PV capacity	kW/house	3.5	4.0	4.0	3.3	5.3	5.0	4.7	5.3	4.2	4.2	4.9	4.4
BTES height-to-width	m/m	5.00	1.32	0.73	3.76	1.19	0.97	1.32	0.89	1.74	3.41	1.04	0.68
BTES volume	m ³ /house	859	286	250	1401	196	247	229	200	411	553	165	359
Borehole density	1/m ²	0.15	0.16	0.16	0.12	0.21	0.20	0.12	0.13	0.21	0.23	0.17	0.15
BTES Insulation	m	0.03	0.10	0.55	0.06	0.04	1.10	0.08	0.21	0.65	0.06	1.19	0.10
Solar tilt	°	53	53	52	53	43	55	43	48	43	50	49	49
Building quality	–	7	7	7	7	7	7	5	7	7	7	5	7
Number of heat pumps	–	2	1	1	3	2	2	5	4	5	14	12	12
BTES width	m	22	24	28	36	28	32	35	38	39	47	47	69
BTES height	m	111	32	20	136	33	31	47	34	68	160	48	47
Number of boreholes	–	60	72	99	120	124	159	118	146	255	392	291	564
Boreholes in series	–	3	6	9	3	2	3	2	2	3	2	1	3
Boreholes/house	–	1.20	1.44	1.98	1.20	1.24	1.59	0.59	0.73	1.28	0.78	0.58	1.13

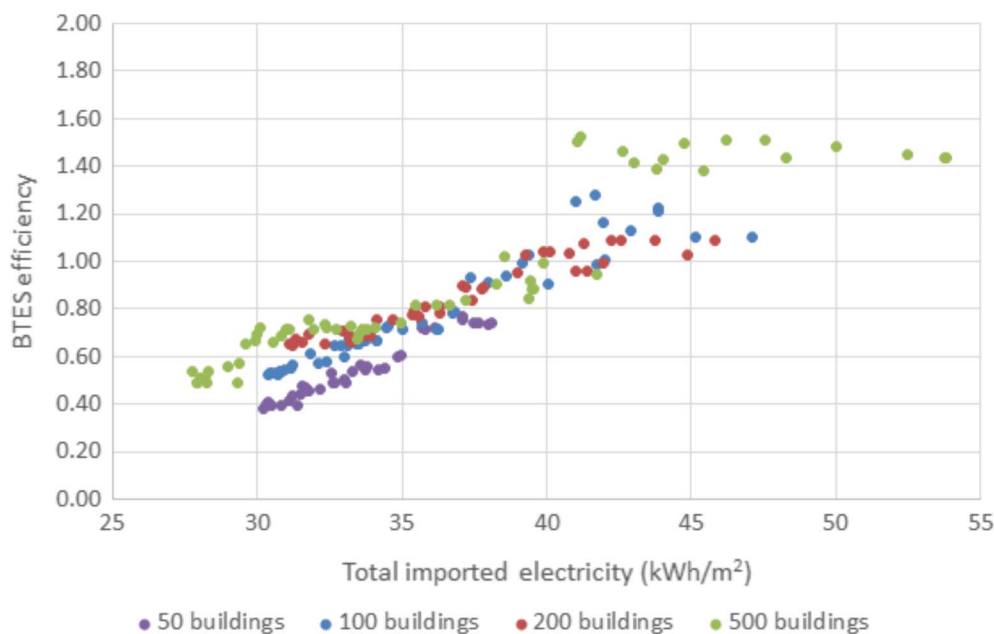


Fig. 9. Average BTES efficiency over the whole lifetime. BTES efficiency was defined as the ratio of discharged vs. charged energy.

decreased while performance improved. This implies that high performance is achieved by having many shallow boreholes on a wide area.

The fraction of heating provided directly from the BTES without HP is shown in Fig. 17. It can be seen that only systems above a certain minimum performance threshold could provide any direct use of the seasonally stored heat. Without enough solar heating capacity, the temperature in the boreholes never rises high enough and thus the heat pump needs to be utilized. The lower temperatures will lower heat losses, while the use of the heat pump will increase the fraction of utilized heat, thus improving BTES efficiency (Fig. 9). The maximum bypass fraction for the 50 and 100 building communities were 0.20 and 0.15 respectively, while with 200 and 500 buildings it was 0.43. Thus, with a larger community, the need for heat pump utilization was lower, but increasing the size from 200 to 500 did not provide additional benefit.

All the optimal solutions had varying solar thermal and seasonal

storage capacities. Fig. 18 shows the renewable energy fraction of heating vs. the ratio of BTES volume to solar collector area (storage-to-generation). REF_{heat} values below 0.74 were obtained by a wide range of storage-to-generation ratios. However, when the storage-to-generation ratio was below 20, a roughly linear trend could be observed, as a decreasing ratio was correlated with an increasing REF_{heat}. The performance values of all community sizes were mixed together and no size effects could be inferred, though in the low REF_{heat} cases the 500 building community had higher relative storage volumes than the other sizes. A cluster of high renewable energy fractions for all sizes can be seen where the storage-to-generation ratio is between 5 and 10. This ratio could be used as a simple design rule when planning a system with high intended use of solar energy.

Ignoring performance values, Fig. 19 shows the relative seasonal storage and solar thermal capacities for all the optimal cases. The corresponding values from realized solar communities were also added

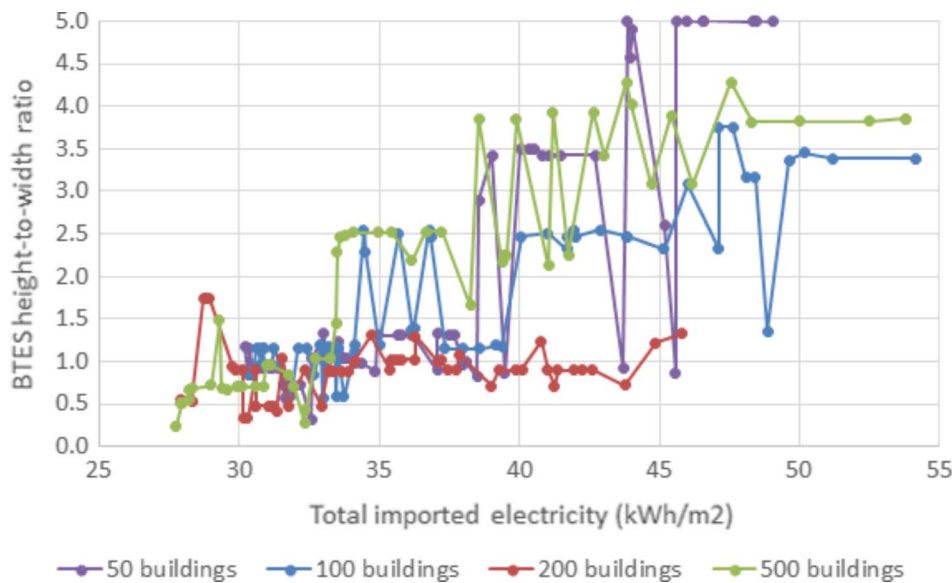


Fig. 10. Height-to-width ratio of BTES for the optimal cases.

for comparison. Most realized cases had values similar to those reached in the optimization, except for Braedstrup (which was designed for a low solar fraction) and Anneberg (which had the highest solar fraction of the real cases but had no heat pump). When the ST area in the simulated cases was very low, it was compensated for with a large BTES volume. In these regions, each size category clustered in different ST capacity ranges, so they are not directly comparable, but the relative storage volume decreased as generation increased. When the ST area exceeded 13 m^2 , all community sizes tended to have storage volumes close to $2 \text{ m}^3/\text{m}^2$. The smallest community size had the highest solar thermal capacities, which points to less efficient seasonal storage, as thermal losses need to be compensated with more generation. This only applies to the high performance group, however, as shown in Fig. 13. Energy performance was strongly tied to the solar thermal area, but in the low performance regions (energy demand over $40 \text{ kWh}/\text{m}^2$) each size category had different approaches to total performance, as evidenced by varying solar thermal areas.

General trends for short-term storage tanks can be seen in Fig. 20. All community sizes show a similar trend, where more than 2 m^3 of buffer storage was only needed to keep purchased electricity demand below $35 \text{ kWh}/\text{m}^2$. The standard deviation for the tank sizes was greatest between demand from 30 to $35 \text{ kWh}/\text{m}^2$. In most cases the warm tank was larger than the hot tank. This was to be expected, as

most of the solar energy was stored in the low temperature tank. In fact, an even larger difference in tank sizes was expected, because roughly 70% of the thermal energy demand was estimated to be met through the low temperature tank. Thus a size difference as high as 130% could be expected. However, the average size difference was 70%, 1%, 30% and 35% for the community sizes of 50, 100, 200 and 500 buildings, respectively. The small difference may indicate some need to adjust temperature set points or charge control algorithms.

The total combined area of ST collectors and PV panels was limited to 60 m^2 . Fig. 21 shows the area of each collector type for all community sizes in the optimal cases. In most cases, PV panels occupied the majority of the used space and in all cases the total area approached the upper limit. For 50, 100 and 500 buildings, there was a rising trend in ST area after going below $40 \text{ kWh}/\text{m}^2$ import need. Changes in PV area were more random in all scenarios. Self-consumption of PV power was not significantly increased above 3 kW capacity (about 20 m^2), which explains the small differences in area between the best and worst performance. Having a very large PV area was not useful, because the value of exported solar electricity was less than that of self-consumed electricity. On average, the best performance was obtained with a near-even split between the two solar collector types.

The LCC was comprised of initial investment costs and lifetime operation costs. Operation cost includes only electricity purchased

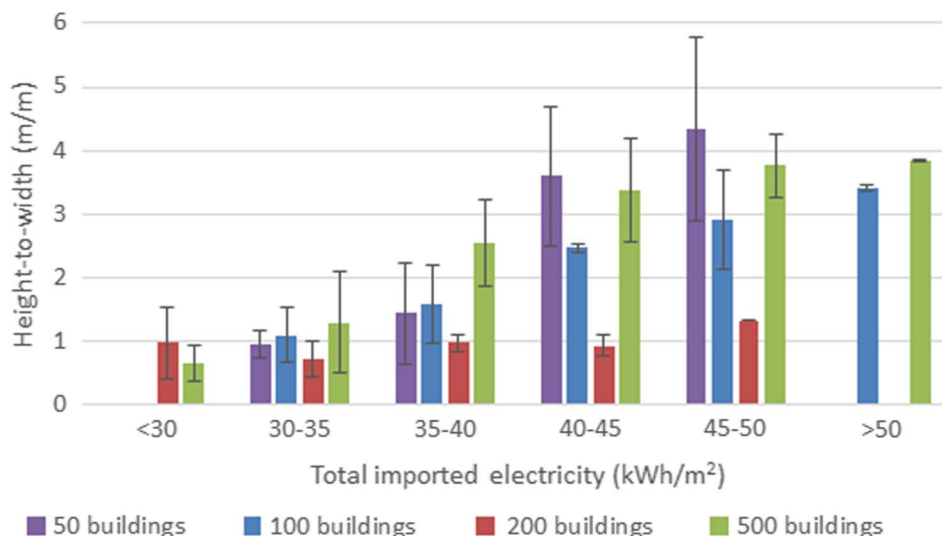
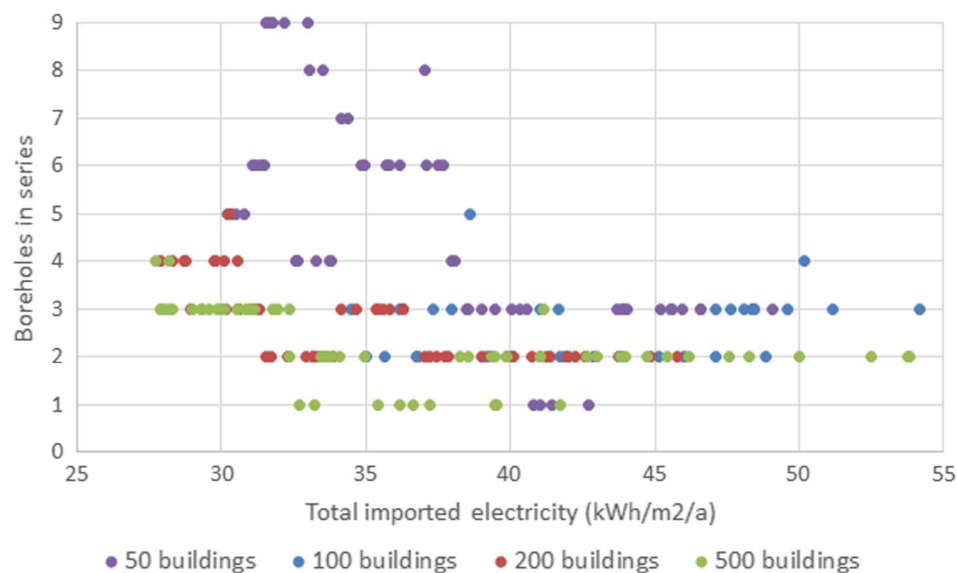
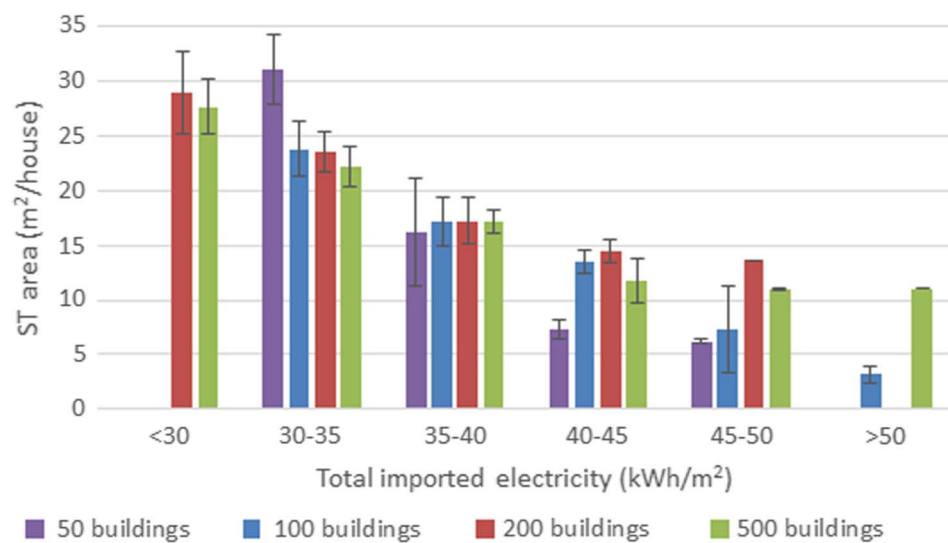
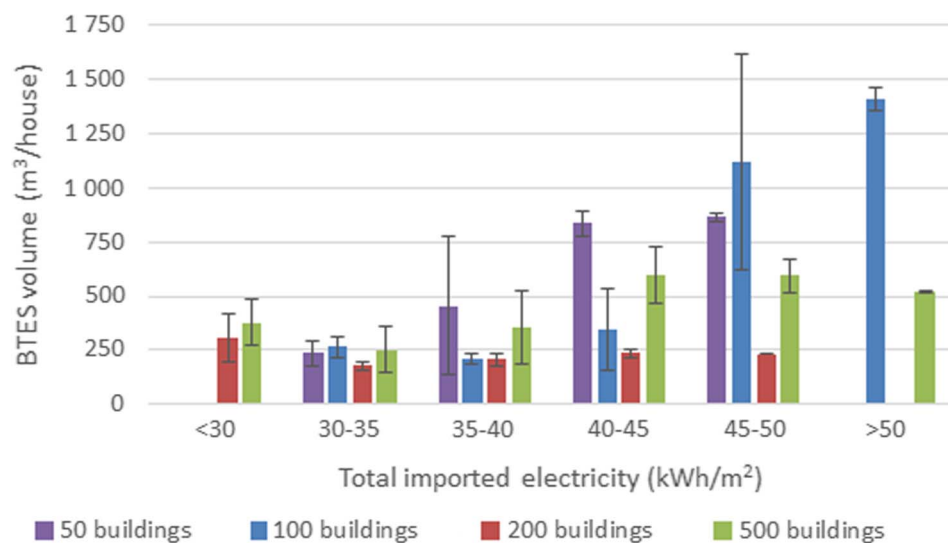


Fig. 11. Height-to-width ratio of BTES for the optimal cases, averaged based on total purchased electricity consumption.



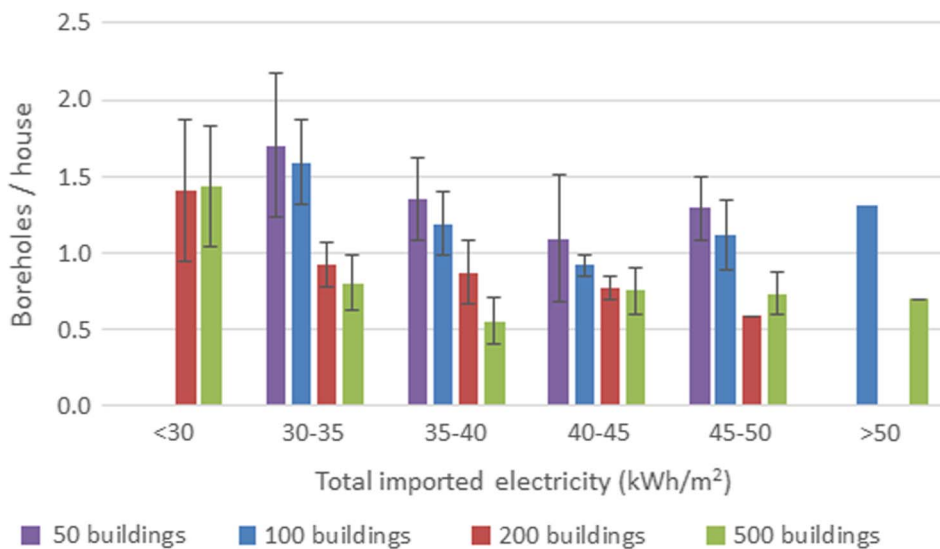


Fig. 15. Average number of boreholes per building in each performance category.

during the 25 years of operation, but no maintenance. Fig. 22 displays the cost distribution for some optimal cases, chosen to have similar total costs (Table 5). In the cheapest category A, the 200 building case had increased heating electricity demand compared to the 50 and 100 building cases. A noticeable difference was a larger investment to ST capacity and a smaller investment to seasonal storage. Investment to PV systems stayed roughly the same for all categories, because self-consumption potential limited the maximum sensible amount of solar electricity, since the selling price of excess electricity was significantly lower than the value of self-consumption. Higher performance of categories B and C was fueled by increased investments to buffer tanks and solar thermal capacity, but also to BTES system in category C.

All the previous results have focused on the total electricity consumption, which includes both the appliances and the heating system. However, to better understand the solar energy system's true performance, one should examine the heating energy separately. Fig. 23 shows how the heating system used electricity in the optimal cases of the 500 building scenario. The electricity demand of the heating system reduced from over 25 kWh/m² in the worst case to 5 kWh/m² in the best case, an 80% reduction. In the low performance cases with little solar energy, the heat pump required significant support from the backup heating system. As the solar thermal area increased, more of the heating demand could be directly met by solar energy, but additionally

the COP of the heat pump was improved and the use of the HP bypass was increased.

4. Discussion

Almost all of the optimal cases included the best-performing building configuration, number 7. This means that reducing heating demand is perhaps the most important step in high latitude solar community design. Saving energy seems to be more cost-effective than adding more generation, especially considering the significant losses entailed in seasonal thermal storage.

The optimal amount of series-connected boreholes in the BTES was lower than expected. In most optimal cases in the 100, 200 and 500 building scenarios, only 1 to 3 boreholes were connected in series, while in the Drake Landing Solar Community it was 6 (Sibbitt et al., 2011). However, in the 50 building case typical values were between 4 and 9. The DLSC community consists of 52 houses, so the results are in line with practical implementation. It seems that having many boreholes connected in series is only important for relatively small communities.

As flowrate within each borehole loop was kept constant, having less seriality increased the amount of separate loops and thus the total flowrate through the BTES. The higher total flow increased both the

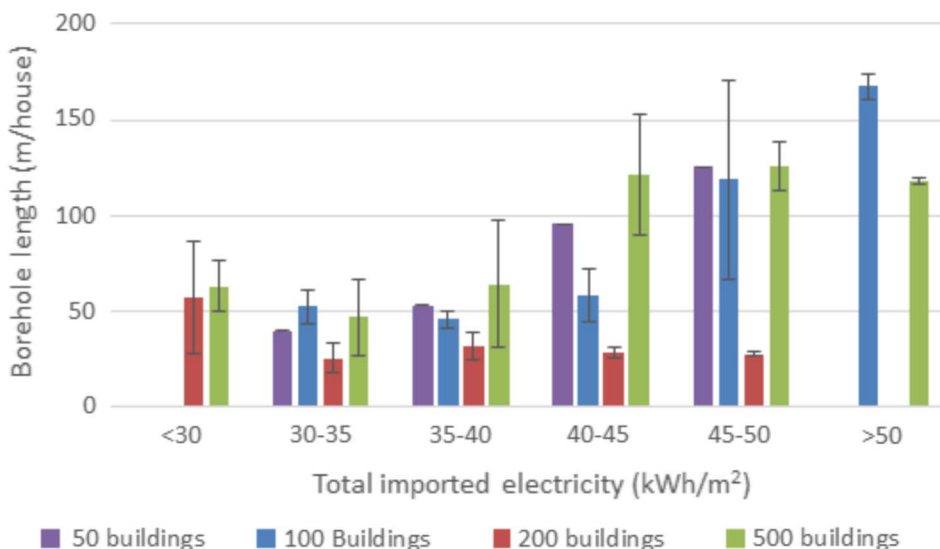


Fig. 16. Average total borehole length per building in each performance category.

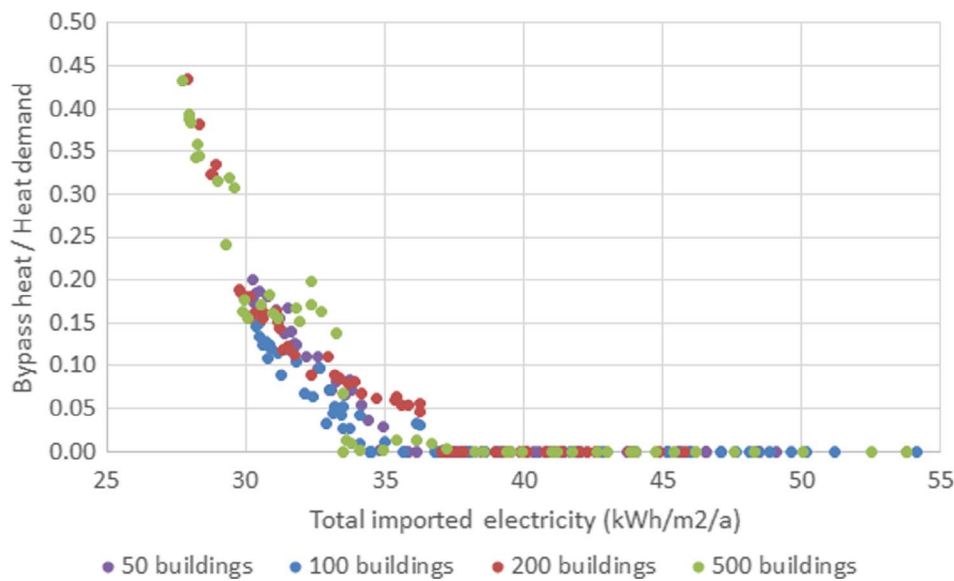


Fig. 17. The fraction of heat provided directly from BTES, bypassing the heat pump.

general performance and the fraction of heat demand met directly by the BTES without the heat pump. Simply increasing the flowrate per pipe circuit should have a similar effect. A constant flowrate was used for discharging the BTES, but it might be beneficial to adjust the flowrate according to the current BTES and tank temperatures.

4.1. Comparison to other studies

The achieved renewable energy fractions in this Finnish simulation study were very favorable compared to some actual German solar communities, as shown in Table 6. Even the low performance cases exceeded in REF_{heat} (solar fraction) both the Neckarsulm and Crailsheim communities. The main difference in this study to the Neckarsulm community is the heat pump. With the help of a heat pump, high

renewable energy fractions can be achieved, even without solar thermal capacity. However, the Crailsheim community also contained a heat pump. The difference between the better performing cases (100C and 500C) and Crailsheim can partly be attributed to the higher solar thermal area compared to heat demand, but it is not the sole reason. The solar capacity to demand ratio was double for 500C compared to Crailsheim, but of the same scale for case 500A. The BTES volume vs demand ratio was 5 times higher for 500C than for Crailsheim. However, even in the lower performance case 500A the REF was significantly higher for the simulated case compared to Crailsheim. Configurations in this study were optimized, so the results can reasonably be expected to be better than those from non-optimal studies. However, no cost comparison vs. Neckarsulm and Crailsheim was done and it is not known what the ratio of cost vs. performance is. Regardless,

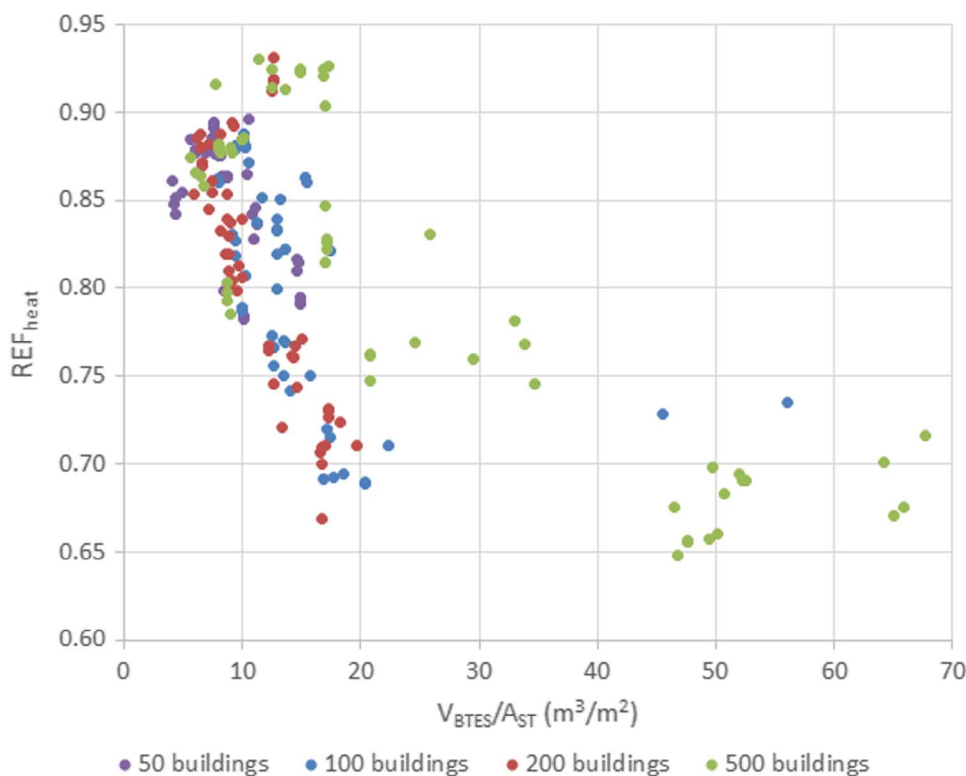


Fig. 18. Renewable energy fraction of heating vs. storage volume to collector area ratio.

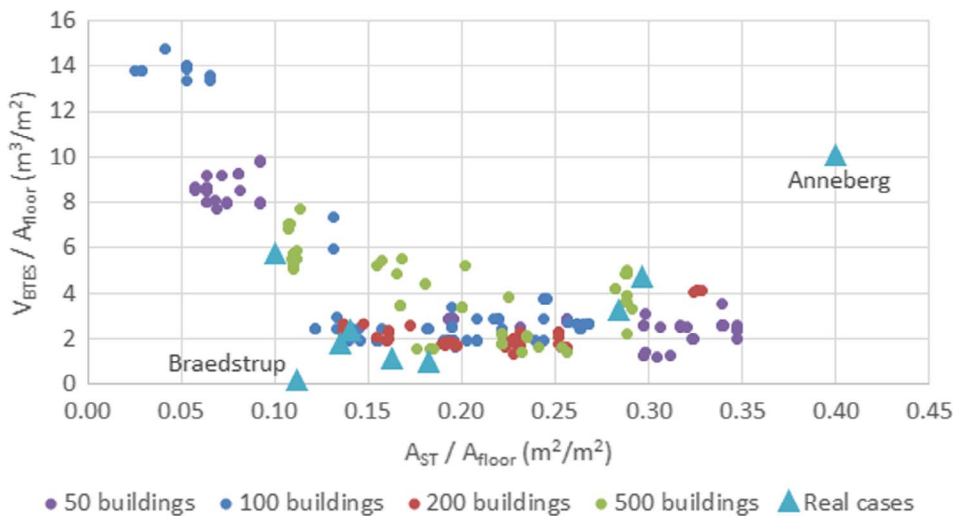


Fig. 19. Relative BTES volume and solar thermal area for each community size. Values from realized solar communities (Fig. 1b) are shown for comparison.

simulated studies are sure to be overly optimistic as real systems always suffer from unexpected problems, such as component failures, less than ideal efficiencies, uncontrolled ground water flows and different than expected environmental conditions. Such technical problems and non-ideal behaviour have been studied in (Rehman et al., 2018).

Another relevant case for comparison is the Drake Landing Solar Community in Canada, which reports the measured performance of their energy system every month (Drake Landing Solar Community Drake, 2012). On year 2012, the DLSC achieved a high solar fraction, which is why the year was chosen for comparison with the Finnish case in this study. From this study, case 100C (year 3) was chosen, due to similarity to the DLSC case. Fig. 24 shows the heating energy used in the district loop, relative to heated floor area. The simulated Finnish case had higher total and summertime values because it included both space heating and domestic hot water demand, while the DLSC case only included space heating. The simulated system utilized very high efficiency buildings, which additionally used low temperature space heating (35–40 °C), while DLSC used higher temperatures (37–55 °C). This can partly explain why the demand in the more northern Finnish location was less than in DLSC. Of course, annual weather differences will also significantly affect the performance.

Fig. 25 shows the incident and collected solar energy for both the simulated and real system. The Finnish case had a lower solar insolation and collection rate, as well as a lower solar thermal efficiency (26% vs

33%). A major difference between the locations is the winter solar potential. While the DLSC produced useful amounts of solar energy even in winter, solar generation in the Finnish case was reduced to almost zero during the November–January period. Collected solar energy vs. collector area was 42% lower in the Finnish case.

Fig. 26 shows the energy used to charge the seasonal storage in the simulated (24,700 m³ BTES volume) and real (34,000 m³ BTES volume) systems. The charge profiles closely followed the solar profiles from Fig. 25 in both cases. The BTES efficiency was 56% in the Finnish case and 50% in the DLSC. More energy relative to volume was injected and discharged in the Finnish case, but in absolute terms the values were similar. The Finnish case had significantly higher discharge rates during the January–March period, due to lower active solar input compared to the DLSC.

5. Conclusions

Multiobjective optimization of a solar district heating system with seasonal thermal energy storage was done for four different community sizes. Based on the Pareto optimal results, large solar communities with 200 and 500 houses could reach lower LCC per floor area than the small communities of 50 and 100 houses, but actual performance was not significantly different in the four size categories. The range for the annual purchased electricity demand with respect to heated floor area

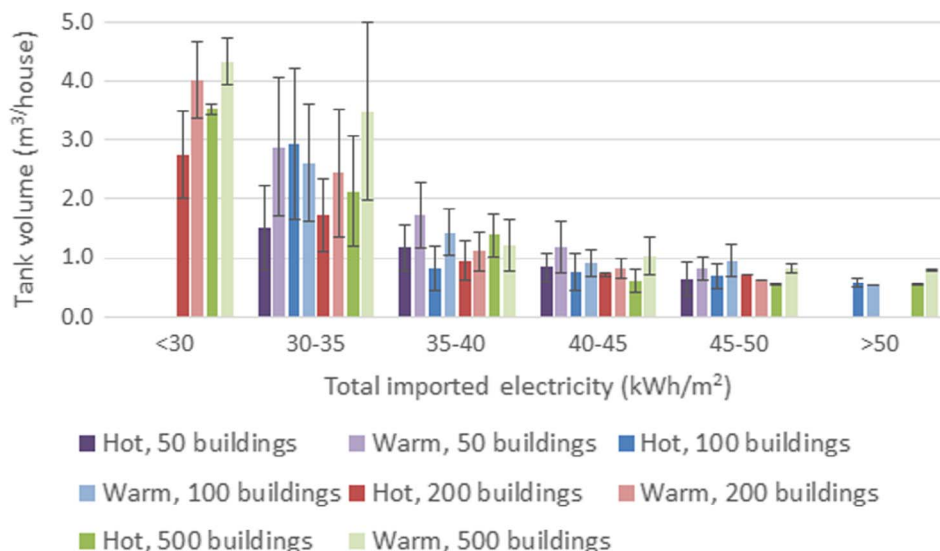


Fig. 20. Average sizes of short-term storage tanks in each performance category.

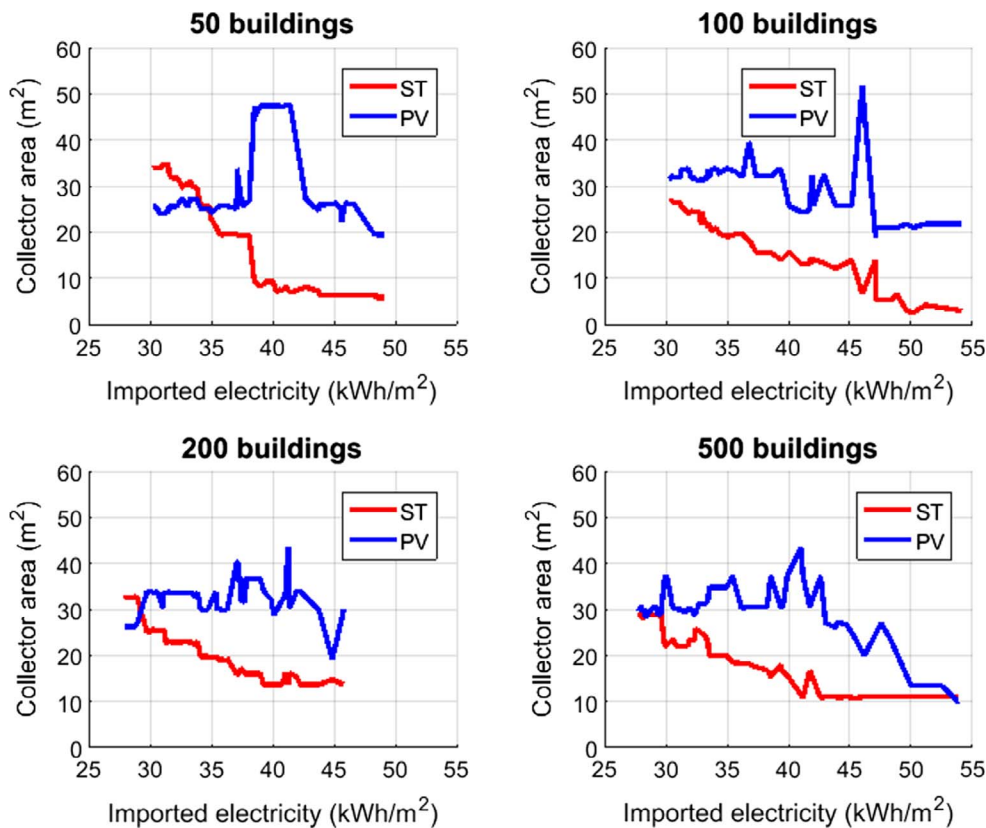


Fig. 21. The use of roof area by ST collectors and PV panels in the optimal cases of each community size.

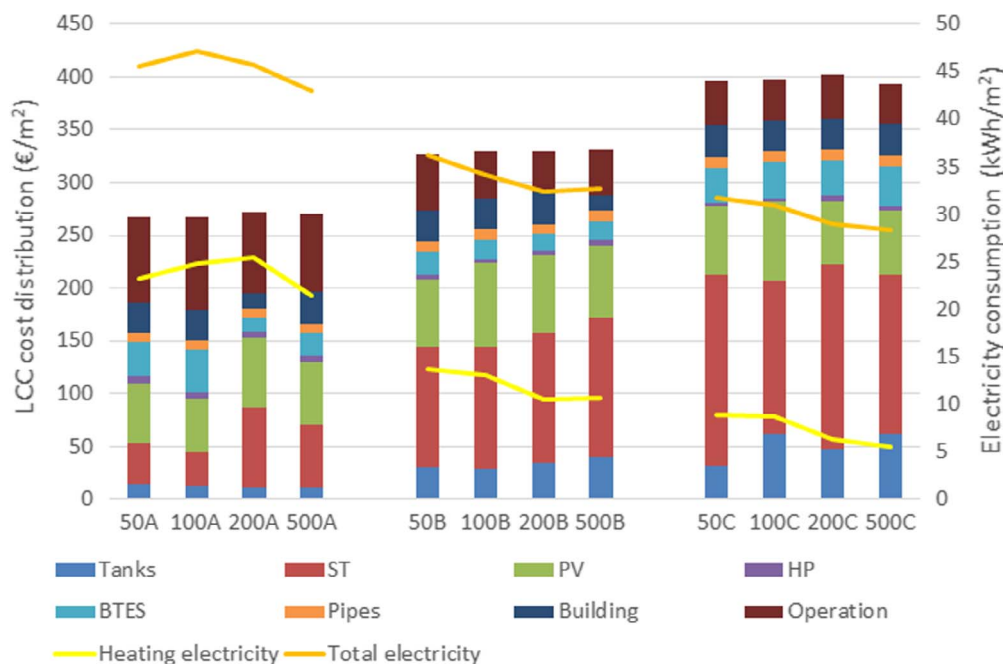


Fig. 22. The distribution of relative lifetime costs between different components for cases with similar LCC. Also shown is the annual electricity used for heating, as well as the total purchased electricity consumption. The letters A, B and C refer to the community cost category, from cheapest to most expensive, as shown in Table 5. The largest communities can be seen to have somewhat lower electricity consumption in each cost category.

was 30–54 kWh/m² for 50 buildings, 30–54 kWh/m² for 100 buildings, 28–46 kWh/m² for 200 buildings and 28–54 kWh/m² for 500 buildings. The life cycle cost ranges for these same cases were 477–259 €/m² for 50 buildings, 420–252 €/m² for 100 buildings, 456–273 €/m² for 200 buildings and 453–260 €/m² for 500 buildings, over a period of 25 years.

The high temperature requirements of DHW demand made the inclusion of a heat pump a necessity for all community sizes. However, a clear benefit from larger community size was related to BTES

performance. In the 200 and 500 building communities the BTES could provide as much as 44% of the required heating directly without utilizing the heat pump, while the 50 and 100 building communities were limited to less than 20%. Electricity consumption of heating systems was reduced by 80% when comparing the best performing optimal cases with those of the lowest cost.

Lowering heating demand through well insulated buildings with heat recovery systems was a high priority, as it was simpler and cheaper than adding more generation and storage capacity. Apartment buildings

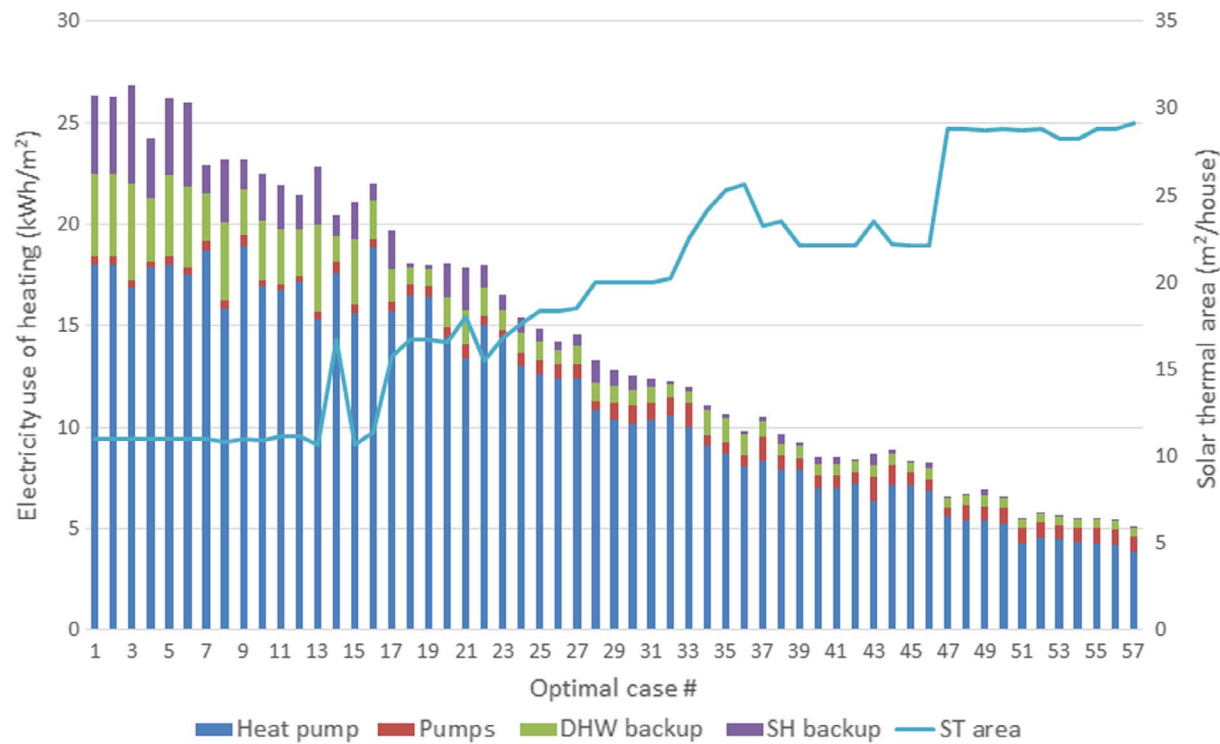


Fig. 23. The distribution of electricity used for heating in the optimal solutions of the 500 building scenario.

Table 6
Comparison to other studies (Nussbicker et al., 2004; Schmidt and Mangold, 2006).

	100A	100C	500A	500C	Neckarsulm (BTES + boiler)	Crailsheim (BTES + HP)
Heat demand (MW h/a)	709	723	3554	3615	1891	4100
ST area (m ²)	531	2637	5569	14 372	5007	7300
BTES volume (m ³)	140 078	24 702	276 588	179 497	63 360	37 500
ST/Heat (m ² /MW h)	0.75	3.65	1.57	3.98	2.65	1.78
BTES/Heat (m ³ /MW h)	197.4	34.2	77.8	49.7	33.5	9.1
REF _{heat}	65	88	70	92	39	50

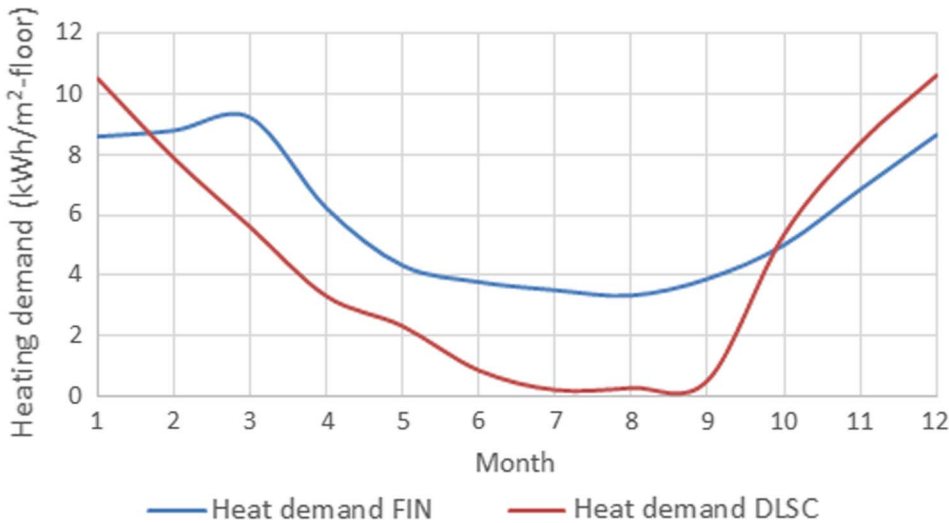


Fig. 24. Heating demand relative to heated floor area in the simulated Finnish case 100C (10 000 m² heated area) and the real Drake Landing Solar Community (11 600 m² heated area) in Canada. Finnish demand includes both DHW and SH, while DLSC includes only SH.

generally have more favorable ratio of external heat transfer area to living space than detached houses. If enough space is available for solar thermal installation, it might offer a solution to further reduce energy demand to obtain high renewable energy fractions more cost-effectively.

High seriality in the borehole connections of the BTES was important for the smallest community of 50 buildings, in which 4 to 9 boreholes were connected in series in the optimal configurations. In other sizes it was less beneficial, as often only 3 or less boreholes were connected in series. Further study on the effect of flowrate on optimal

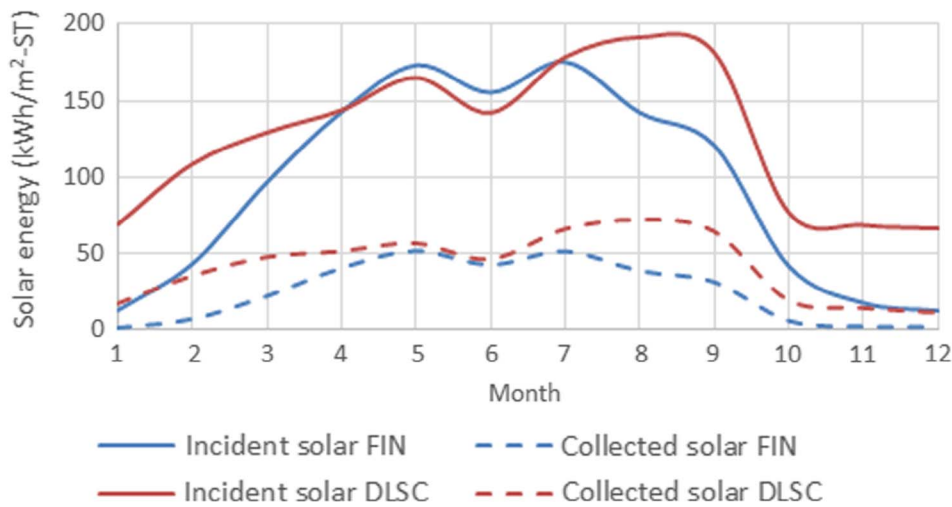


Fig. 25. Incident and collected solar energy for the simulated case 100C (2640 m² collector area) and the real DLSC (2293 m² collector area).

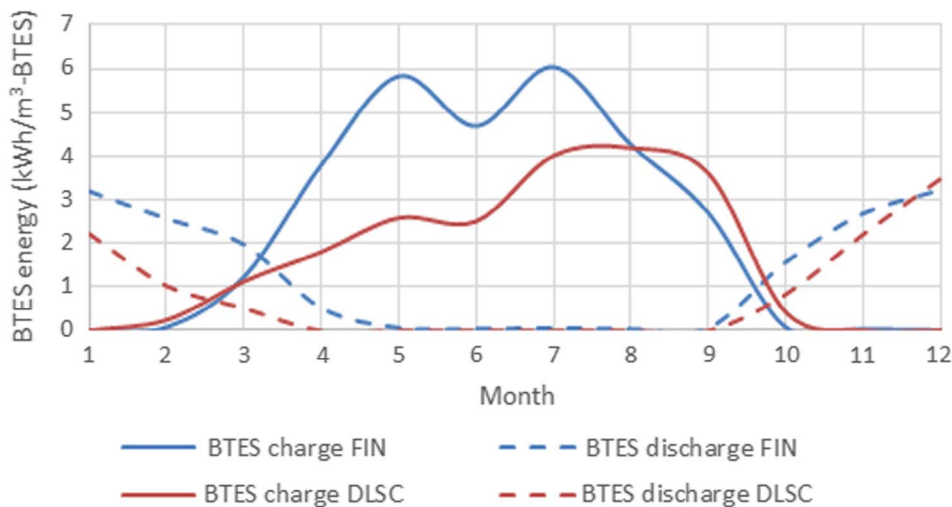


Fig. 26. Energy transfer to and from the BTES in the simulated case 100C (24 700 m³ BTES volume) and the real DLSC (34 000 m³ BTES volume).

borehole connectivity is required.

This study has shown that solar thermal energy can be used to provide a significant fraction of winter heating even in high latitude Nordic countries. Larger systems reduce unit costs while increasing the potential of seasonal storage. However, more realized projects are needed to generate practical experience on system design and operation and to lower costs through increased market activity.

Acknowledgements

The authors are grateful for the funding provided by the Academy of Finland through the New Energy research program.

References

- Ahola, J., 2015. National survey report of PV power applications in Finland. Tech. rep., International Energy Agency.
- Bauer, D., Marx, R., Nulbicker-Lux, J., Ochs, F., Heidemann, W., Müller-Steinhagen, H., 2010. German central solar heating plants with seasonal heat storage. *Sol. Energy* 84, 612–623.
- Cao, S., Hasan, A., Sirén, K., 2013. On-site energy matching indices for buildings with energy conversion, storage and hybrid grid connections. *Energy Build.* 64, 423–438.
- Caruna, 2016. Electricity distribution prices [In Finnish]. <<https://www.caruna.fi/hinnat>>.
- Drake Landing Solar Community, 2012. Reports: DLSC. <<https://www.dlsc.ca/reports.htm>>.
- EU-Commission, 2012. Commission delegated regulation c(2011) 10050. <<http://ec.europa.eu/transparency/regdoc/rep/3/2011/EN/3-2011-10050-EN-F1-1.Pdf>>.
- Finlex, 2007. D1 Finnish building directives [In Finnish]. <http://www.finlex.fi/data/normit/28208/D1_2007.pdf> (accessed 9.1.2017).
- Flynn, C., Sirén, K., 2015. Influence of location and design on the performance of a solar district heating system equipped with borehole seasonal storage. *Renewable Energy* 81, 377–388.
- Fortum Oy, 2015. Fortum company website. <<https://www.fortum.com/>>.
- Hahtela, Y., Kiiras, J., 2013. Talonrakennuksen kustannustieto 2013 [in Finnish] (Building Construction Cost Data 2013). Hahtela-kehitys.
- Hamdy, M., Hasan, A., Sirén, K., 2013. A multi-stage optimization method for cost-optimal and nearly-zero-energy building solutions in line with the EPBD-recast 2010. *Energy Build.* 56, 189–203.
- Hamdy, M., Palonen, M., Hasan, A., 2012. Implementation of Pareto-archive NSGA-II algorithms to a nearly-zero-energy building optimisation problem. In: First Building Simulation and Optimization Conference. <<http://www.ibpsa.org/proceedings/BSO2012/3A3.pdf>>.
- Heller, A., 2000. 15 years of R&D in central solar heating in Denmark. *Sol. Energy* 69, 437–447.
- Hirvonen, J., Kayo, G., Hasan, A., Sirén, K., 2016. Zero energy level and economic potential of small-scale building-integrated PV with different heating systems in Nordic conditions. *Appl. Energy* 167 (1), 255–269 April.
- Jordan, U., Vajen, K., 2001. Realistic domestic hot-water profiles in different time scales. Tech. rep., International Energy Agency, Task 26.
- Kalamees, T., Jylhä, K., Tietäväinen, H., Jokisalo, J., Ilomets, S., Hyvönen, R., Saku, S., 2012. Development of weighting factors for climate variables for selecting the energy reference year according to the EN ISO 15927-4 standard. *Energy Build.* 47 (0), 53–60. <<http://www.sciencedirect.com/science/article/pii/S0378778811005779>>.
- Lund, P., 1984. Optimization of a community solar heating system with a heat pump and seasonal storage. *Sol. Energy* 33, 353–361.
- Lundh, M., Dalenbäck, J.-O., 2008. Swedish solar heated residential area with seasonal storage in rock: initial evaluation. *Renewable Energy* 33, 703–711.
- Mauthner, F., 2016. Task 52 - C1: Classification and benchmarking of solar thermal systems in urban environments. Tech. rep., International Energy Agency, Solar Heating and Cooling Programme.
- Modi, A., Bühler, F., Andreasen, J.G., Haglind, F., 2017. A review of solar energy based heat and power generation systems. *Renew. Sustain. Energy Rev.* 67, 1047–1064.

- Nord Pool, 2016. Nord Pool electricity prices. <<https://www.nordpoolspot.com/Market-data1/Elspot/Area-Prices/EL/Yearly/?view=table>> (accessed 24.8.2016).
- Nussbicker, J., Mangold, D., Heidemann, W., Müller-Steinhagen, H., 2004. Solar assisted district heating system with seasonal duct heat store in Neckarsulm-Amorbach (Germany). In: EuroSun 2004.
- Palonen, M., Hamdy, M., Hasan, A., 2013. MOBO, a new software for multi-objective building performance optimization. In: 13th Conference of International Building Performance Association. <http://www.ibpsa.org/proceedings/BS2013/p_1489.pdf>.
- Rakennuslehti, 2016. Prices for construction work in Helsinki region [in Finnish]. Construction-related magazine.
- Ramboll, 2015. South-Jutland stores the sun's heat in the world's largest pit heat storage. <<http://www.ramboll.com/projects/re/south-jutland-stores-the-suns-heat-in-the-worlds-largest-pit-heat-storage>> (accessed 10.1.2017).
- Rautia, 2016. Price of polystyrene thermal insulation for soil layers. <<https://www.rautia.fi/verkkokauppa/rakennustarvikkeet-ja-puutavara/rakennustarvikkeet/eps-eristeet/eristyslevy-thermisol-eps-120-routa-50x1000x1200mm-12m2>> (accessed 13.6.2016).
- Rehman, H., Hirvonen, J., Sirén, K., 2018. Influence of technical failures on the performance of an optimized community-size solar heating system in Nordic conditions. *J. Cleaner Prod.* 175, 624–640. <<http://www.sciencedirect.com/science/article/pii/S0959652617330238>>.
- Reuss, M., 2015. *Advances in Thermal Energy Storage Systems – Methods and Applications*. Woodhead Publishing.
- Reuss, M., Beuth, W., Schmidt, M., Schoelkopf, W., 2006. Solar district heating with seasonal storage in Attenkirchen. In: ECOSTOCK. 10th International Conference on Thermal Energy Storage, 2006. <https://intraweb.stockton.edu/eyos/energy_studies/content/docs/FINAL_PAPERS/6B-2.pdf>.
- Schmidt, T., Mangold, D., 2006. New steps in seasonal thermal storage in Germany. In: Ecstock 2006. <https://intraweb.stockton.edu/eyos/energy_studies/content/docs/FINAL_PAPERS/14A-2.pdf>.
- Schmidt, T., Mangold, D., Müller-Steinhagen, H., 2004. Central solar heating plants with seasonal storage in Germany. *Sol. Energy* 76, 165–174.
- SDH EU, 2012. Braedstrup solar community. <<http://solar-district-heating.eu/NewsEvents/News/tabid/68/ArticleId/216/Braedstrup-Solar-Park-in-Denmark-is-now-a-reality.aspx>> (accessed 3.1.2017).
- Sibbitt, B., McClenahan, D., Djebbar, R., Thornton, J., Wong, B., Carriere, J., Kokko, J., 2011. The performance of a high solar fraction seasonal storage district heating system – five years of operation. *Energy Procedia*.
- Solar Keymark Database, 2013. Solar collector datasheet, SF 100-01A-Ruukki. <http://www.estif.org/solarkeymark/Links/Internal_links/certif/PSK-042-2013.pdf>.
- Statistics Finland, 2014. Energy consumption in households 2010–2014. <http://www.stat.fi/til/asen/2014/asen_2014_2015-11-20_tau_001_en.html> (accessed 21.12.2016).
- Tulus, V., Boer, D., Cabeza, L.F., Jiménez, L., Guillén-Gosálbez, G., 2016. Enhanced thermal energy supply via central solar heating plants with seasonal storage: a multi-objective optimization approach. *Appl. Energy* 181, 549–561.
- Xu, J., Wang, R., Li, Y., 2014. A review of available technologies for seasonal thermal energy storage. *Sol. Energy* 103, 610–638.
- Zhu, X., 2014. Exploring the possibility of applying seasonal thermal energy storage in south-west of China. Bachelor's thesis.